

Numerical Prediction of Shear Flows by Upwind Methods

Original

Numerical Prediction of Shear Flows by Upwind Methods / Pandolfi, M., D'Ambrosio, D.. - ELETTRONICO. - (2001), pp. 139-144. (First International Conference on Computational Fluid Dynamics, Kyoto, Japan Kyoto, Japan 10-14 July, 2000) [10.1007/978-3-642-56535-9_18].

Availability:

This version is available at: 11583/1410830 since: 2024-01-10T16:57:50Z

Publisher:

Springer

Published

DOI:10.1007/978-3-642-56535-9_18

Terms of use:

This article is made available under terms and conditions as specified in the corresponding bibliographic description in the repository

Publisher copyright

Springer postprint/Author's Accepted Manuscript

This version of the article has been accepted for publication, after peer review (when applicable) and is subject to Springer Nature's AM terms of use, but is not the Version of Record and does not reflect post-acceptance improvements, or any corrections. The Version of Record is available online at: http://dx.doi.org/10.1007/978-3-642-56535-9_18

(Article begins on next page)

Numerical Prediction of Shear Flows by Upwind Methods

Maurizio Pandolfi and Domenic D'Ambrosio

Dipartimento di Ingegneria Aeronautica e Spaziale - Politecnico di Torino
e-mail: pandolfi@polito.it - domenic@athena.polito.it

1 Introduction

Flow fields in high speed regimes exhibit strong shock waves and sharp boundary layers (BL). Their numerical prediction is generally obtained with some of the several upwind methods that have been proposed in the literature over the past twenty years. Though shock waves are computed with a satisfactory numerical capturing, the description of shear flows, such as boundary layers, can suffer of severe shortcomings. These problems have widely experimented more than a decade ago for certain upwind methods and, more recently, for others. In the following we discuss this matter and focus attention on the motivations for such numerical deficiencies.

2 A Significant Problem and Some Numerical Experiments

We consider a simple but significant problem: *the high speed flow over a flat plate in the laminar regime*. Downstream of the front region of strong interaction, just behind the leading edge of the plate, the flow field structure is characterized by the viscous region of the BL, closely to the wall. An outer oblique shock wave, induced by the BL obstruction, propagates higher over the plate. Inside the BL, the velocity presents, along the normal to the plate, severe variations, as well as do the density or the temperature. On the contrary, the pressure is very uniform, since the streamlines run almost parallel each other. The diffusive fluxes (typical of the N-S eqs.) play a dominant role inside the BL, by generating the correct physical dissipation and diffusion. On the contrary, the convective fluxes (typical of the Euler eqs.) should be almost inactive and must avoid any spurious injection of numerical (therefore artificial) dissipation, even in the presence of strong variations of the density and the velocity. However, we find that not all the upwind methods give the correct estimate of the convective fluxes and, depending on the upwind method, the thickness of the BL can result anomalously thicker because of the additional numerical dissipation or the pressure distribution inside the BL can show questionable oscillations.

In order to investigate the effects due to the different upwind methods, we have computed the flat plate flow field with a simple code based on the time-dependent

integration of the laws of conservation (laminar N-S), a finite volumes discretization on a properly stretched structured grid and the plain first order scheme. The diffusive fluxes at the interface between two adjacent volumes are evaluated with a centered approximation and the convective fluxes are estimated with several upwind methods that appear in the literature; the first order scheme is adopted to emphasize the features of each upwind method.

We classify in groups the upwind methods that we consider in the following numerical experiments: **(a)** flux-difference splitting methods (FDS), with the approximate solvers shown in [15] (FDSROE) and [11] (FDSPAN, a mirror image of the solver proposed in [10]), **(b)** flux-vector splitting methods (FVS) in the version reported in [16] (FVSSW), [19] (FVSVL) and [12] (FVSEFM), **(c)** the method HLL (or HLLE) proposed in [5] and [3], **(d)** the AUSM methods presented in [7] (AUSM-VEL), [8] (AUSM-M) and [9] (AUSM+), and **(e)** methods, FDS mimics, initially different from the FDS ones, that tend to mimic them through some implementations and are discussed in [1] (HUS, based on FVS), [3] (HLLM, based on HLL), [17] (HLLC, also based on HLL), [20] [21] (AUSMD and AUSMV).

We have performed numerical experiments with the above methods by predicting the flow field of the flat plate problem characterized by the following data: length of the plate $L = 1.0m$ and upstream conditions $M_\infty = 5.0$, $Re_{\infty L} = 62,000m^{-1}$, $T_\infty = 72.2K$, $T_w = 300K$ and $Pr = 0.72$. The results, presented as pressure (p/p_∞) distribution on the normal to the plate, at the distance $x = 0,89m$ from the leading edge, are compared with a reference solution obtained with a code that is based on FDSPAN, accurate ENO scheme and a much finer grid, and has been checked against test-cases reported in the literature.

The FDS predictions by FDSROE and FDSPAN, almost coincident, appear superimposed in Fig.1. The shock wave and the expansion fan are not so sharp as they should be, due to the poor accuracy of the first order scheme and the rough grid. Nonetheless, the overall prediction is good. The shock location and the pressure value at the wall are correct: these are indications that the numerical dissipation has been kept low.

The results obtained with the FVS methods are different. Those from FVSSW and FVSVL are shown in Fig.2 and those from FVSEFM and HLL appear in Fig.3. The sharpness of the captured oblique shock is very good for FVSVL and HLL, not so much for FVSSW and FVSEFM, but the most important fact is that its location is too far from the wall and the pressure level there is definitely overestimated. These results are due to a remarkable numerical dissipation injected in the BL.

The results given by the three version of AUSM are reported in Fig.4. The versions, AUSM-VEL and AUSM-M, almost coincident except at the wall, give a sharp capturing of the oblique shock, whereas AUSM+ shows a thicker capturing zone. The pressure level at the wall seems to have been well predicted, a sign that the numerical dissipation is minimal. However, a questionable result is represented by the pressure oscillation inside the BL, in the proximity of the

wall. Such an oscillation shows up clearly for AUSM-VEL, but also, though with smaller amplitude, in AUSM-M and AUSM+, as it could be seen in enlarged scale of the abscissa (Fig.5) or by increasing the Reynolds number.

The results obtained with FDS mimics methods are very close to the FDS ones. We do not report any result from them, but we remark that these methods fully reproduce the FDS features.

The remarkable discrepancies among the numerical predictions in a trivial fluid-dynamic case require a critical interpretation of the algorithms that are dictated by the different upwind methods.

3 A Critical Analysis on Upwind Methods

We borrow here the *odd-even decoupling problem* suggested in [13] in the investigation of numerical instabilities typical of some upwind methods in flows with strong shocks, and we extend that analysis to a more general case and to the many considered upwind methods.

The present analysis starts from the Euler eqs. (upwinding refers to the convective fluxes) in the 2D (x, y) problem, written in the linearized form about the uniform parallel flow characterized by $\rho_0 = 1.0$, $u_0 \neq 0$, $v_0 = 0$, $p_0 = 1.0$ (u and v are the velocity components along x and y). For each upwind method we develop the algorithm within the frame of the above linearization and we estimate the flux on any interface between two adjacent volumes. The flow is assumed uniform along x and variations can only occur on the transversal direction y . Initial conditions are imposed with alternate perturbations along y : $\rho^0 = 1 \pm \hat{\rho}^0$, $u^0 = u_0 \pm \hat{u}^0$, $v^0 = 0$, $p^0 = 1 \pm \hat{p}^0$, where the signs $+$ and $-$ hold alternatively in the cells in the y direction. Then, the first order scheme is constructed and the integration in time is carried out on the basis of the initial conditions (ρ^0, u^0, v^0, p^0) . Finally, it is possible to obtain simple recursive formulas that determine the flow properties at any integration step $K + 1$, starting at the step K . These formulas are reported in Tab.1. The label MOC refers to the FDS approach as originally proposed in [4] and founded on the method of characteristics. The formulas provide the evolution in time of the perturbations of density ($\hat{\rho}$), velocity (\hat{u}) and pressure (\hat{p}).

In order to interpret the results shown in the Figs.1-4, we assume initial perturbations of density and velocity ($\hat{\rho}^0 \neq 0$, $\hat{u}^0 \neq 0$) and uniform pressure ($\hat{p}^0 = 0$), a situation somewhat similar to a BL. The correct solution of the Euler eqs. requires the preservation of the initial conditions. It is now interesting to see how the different upwind schemes react in this problem.

The FDS methods (MOC, FDSROE, FDSPAN) give the correct answer: at any K (and for $K \rightarrow \infty$), we have $\hat{\rho}^\infty = \hat{\rho}^K = \hat{\rho}^0$ and $\hat{u}^\infty = \hat{u}^K = \hat{u}^0$. Therefore, we expect that, in the flat plate problem, the FDS methods do not react to the density and velocity profiles generated by the only diffusive terms of the N-S equations and that the convective terms do not add any incorrect dissipation. The recursive formulas for MOC, the approximate solvers FDSROE and

FDS PAN and the FDS mime HLLC are coincident. Similar results are obtained also for the other FDS mimes (HUS, AUSMD, AUSMV), since the only slight variation appears in the coefficient of the pressure perturbation that remains null in this analysis ($\hat{p}^\infty = \hat{p}^K = \hat{p}^0 = 0$), but the structure of the formulas remains the same.

On the contrary, the reaction of the FVS methods is very different. Even if the coefficients in the formulas are not equal, the structure of the formulas results the same for FVSSW, FVSVL and FVSEFM. The initial perturbations, $\hat{\rho}^0$ and \hat{u}^0 decrease continuously by denoting the generation of spurious numerical dissipation. Also HLL presents the same incorrect behavior, even if the coefficient are different. It is now clear why the thickness of the BL is overestimated in Figs. 2 and 3, as well as the wall pressure: the inviscid fluxes of FVS and HLL methods, inside regions of finite gradients of density and velocity, tend to flatten these gradients by injecting numerical dissipation.

The AUSM methods react differently. If we look at AUSM-VEL, we recognize that the velocity perturbation is preserved correctly, but the density perturbation is amplified and triggers a stable pressure perturbation initially absent: $\hat{p}^\infty = \hat{p}^\infty = \frac{\gamma}{\gamma-1} \hat{\rho}^0$. This very anomalous behavior is confirmed, in computations carried out for the flat plate problem, by the generation of steady pressure oscillations in the BL that are induced by the density gradient, just as shown in Figs. 4 and 5. The recursive formulas for AUSM-M and AUSM+ are identical each other and very simple: any initial perturbation is preserved. This is correct for density and velocity. However, the pressure should change through traveling waves as for FDS, whereas the recursive formulas indicate that they will be maintained. Therefore we shall be not surprised in detecting small but persistent pressure oscillations even with these two methods. We remind that the generation of more or less remarkable pressure oscillations with these methods has been already experimented in computations of practical interest and reported in the literature [14] [18] [6].

References

1. Coquel,F. and Liou.M.S., AIAA Paper 93-3302-CP, 1993.
2. Einfeldt,B.,SIAM J.Numer. Anal., Vol.25, N.2, pp.294,318., 1988.
3. Einfeldt,B., Munz,C.D., Roe,P.L. and Sjögren,B.,*J.C.P.*, Vol.92,1991, pp.273-295.
4. Godunov,S.K.,*Mat.Sb.*, Vol.47, pp.271,290, 1959.
5. Harten,A., Lax,P.D. and Van Leer,B.,*SIAM Review*, Vol.25, N.1, pp.35,61, 1983.
6. Kim,K.H. et al., *Computers and Fluids*, Vol. 29, No.3,pp.311,346, 1998.
7. Liou.M.S.,*Lecture Notes in Physics*, Vol.414, Springer-Verlag, 1993.
8. Liou,M.S. and Steffen,C.J., *J.Comput.Phys.*, Vol.107,, pp.23,39, 1993.
9. Liou,M.S., *J.Comput.Phys.*, Vol. 129, pp.364,382, 1996.
10. Osher,S. and Solomon,F.,*Mathematics of Computations*, Vol.38, 1982, pp.339,377.
11. Pandolfi,M., *AIAA J.*, Vol.22, pp.602,610, 1984.
12. Pullin, *J.Comput.Phys.*, Vol. 34, pp.231,244, 1980.
13. Quirk,J.J., *ICASE Report 92-64*, 1992.
14. Radespiel,R. and Kroll,N., *J.Comput.Phys.*, Vol.121, pp.66,78, 1991.

15. Roe, P.L., *J. Comput. Phys.*, Vol. 43, pp.357,372, 1981.
16. Steger, J.L. and Warming, R.F., *J. Comput. Phys.*, Vol. 40, pp.263,293, 1981.
17. Toro, E.F., Spruce, M., and Speares, W., *Shock Waves*, Vol.4, pp.25,34, 1994.
18. van Keuk, J. et al., *AIAA 8th Int. Hyp. Syst. and Techn. Conf.*, Norfolk, VA, 1998.
19. Van Leer, B., *Lectures Notes in Physics*, Vol 170, Springer-Verlag, 1982.
20. Wada, Y. and Liou, M.S., *NASA T.M. 106452*, 1994.
21. Wada, Y. and Liou, M.S., *SIAM J.Sci. Comput.*, Vol.18, N.3, pp.633,657, 1997.

Table 1. Integration with the linearized form of the different methods.

MOC	$\hat{\rho}^{K+1} =$	$\hat{\rho}^K$	+	$(-\frac{2\nu}{\gamma})\hat{p}^K$
FDSROE	$\hat{u}^{K+1} =$	\hat{u}^K		
FDSPAN	$\hat{p}^{K+1} =$	$(1 - 2\nu)\hat{p}^K$		
HLLC				
FVSSW	$\hat{\rho}^{K+1} =$	$(1 - \frac{\nu}{\gamma})\hat{\rho}^K$	+	$(-\frac{\nu}{\gamma})\hat{p}^K$
	$\hat{u}^{K+1} =$	$(1 - \frac{2\nu}{\gamma})\hat{u}^K$		
	$\hat{p}^{K+1} =$	$(\frac{\nu}{\gamma})\hat{p}^K$		
FVSVL	$\hat{\rho}^{K+1} =$	$(1 - \frac{\nu}{2})\hat{\rho}^K$	+	$(-\frac{\nu}{2})\hat{p}^K$
	$\hat{u}^{K+1} =$	$(1 - 2\nu)\hat{u}^K$		
	$\hat{p}^{K+1} =$	$(\nu \frac{\gamma}{\gamma + 1})\hat{p}^K$		
FVSEFM	$\hat{\rho}^{K+1} =$	$(1 - \frac{\sqrt{2\nu}}{\sqrt{\pi\gamma}})\hat{\rho}^K$	+	$(-\frac{\sqrt{2\nu}}{\sqrt{\pi\gamma}})\hat{p}^K$
	$\hat{u}^{K+1} =$	$(1 - 2 \frac{\sqrt{2\nu}}{\sqrt{\pi\gamma}})\hat{u}^K$		
	$\hat{p}^{K+1} =$	$(\frac{(\gamma + 1)\nu}{\sqrt{2}\sqrt{\pi\gamma}})\hat{p}^K$		
HUS	$\hat{\rho}^{K+1} =$	$\hat{\rho}^K$	+	$(-\frac{\nu}{2} \frac{\gamma + 1}{\gamma})\hat{p}^K$
	$\hat{u}^{K+1} =$	\hat{u}^K		
	$\hat{p}^{K+1} =$	$(1 - \nu \frac{3\gamma - 1}{\gamma + 1})\hat{p}^K$		
HLL	$\hat{\rho}^{K+1} =$	$(1 - 2\nu)\hat{\rho}^K$		
	$\hat{u}^{K+1} =$	$(1 - 2\nu)\hat{u}^K$		
	$\hat{p}^{K+1} =$	$(1 - 2\nu)\hat{p}^K$		
AUSM-VEL	$\hat{\rho}^{K+1} =$	$(1 + \frac{\nu}{2})\hat{\rho}^K$	+	$(-\frac{\nu}{2})\hat{p}^K$
	$\hat{u}^{K+1} =$	\hat{u}^K		
	$\hat{p}^{K+1} =$	$(\frac{\nu\gamma}{2})\hat{p}^K$		
AUSM-M	$\hat{\rho}^{K+1} =$	$\hat{\rho}^K$		
AUSM+	$\hat{u}^{K+1} =$	\hat{u}^K		
	$\hat{p}^{K+1} =$	\hat{p}^K		
AUSMD	$\hat{\rho}^{K+1} =$	$\hat{\rho}^K$	+	$(-\nu)\hat{p}^K$
AUSMV	$\hat{u}^{K+1} =$	\hat{u}^K		
	$\hat{p}^{K+1} =$	$(1 - \nu\gamma)\hat{p}^K$		

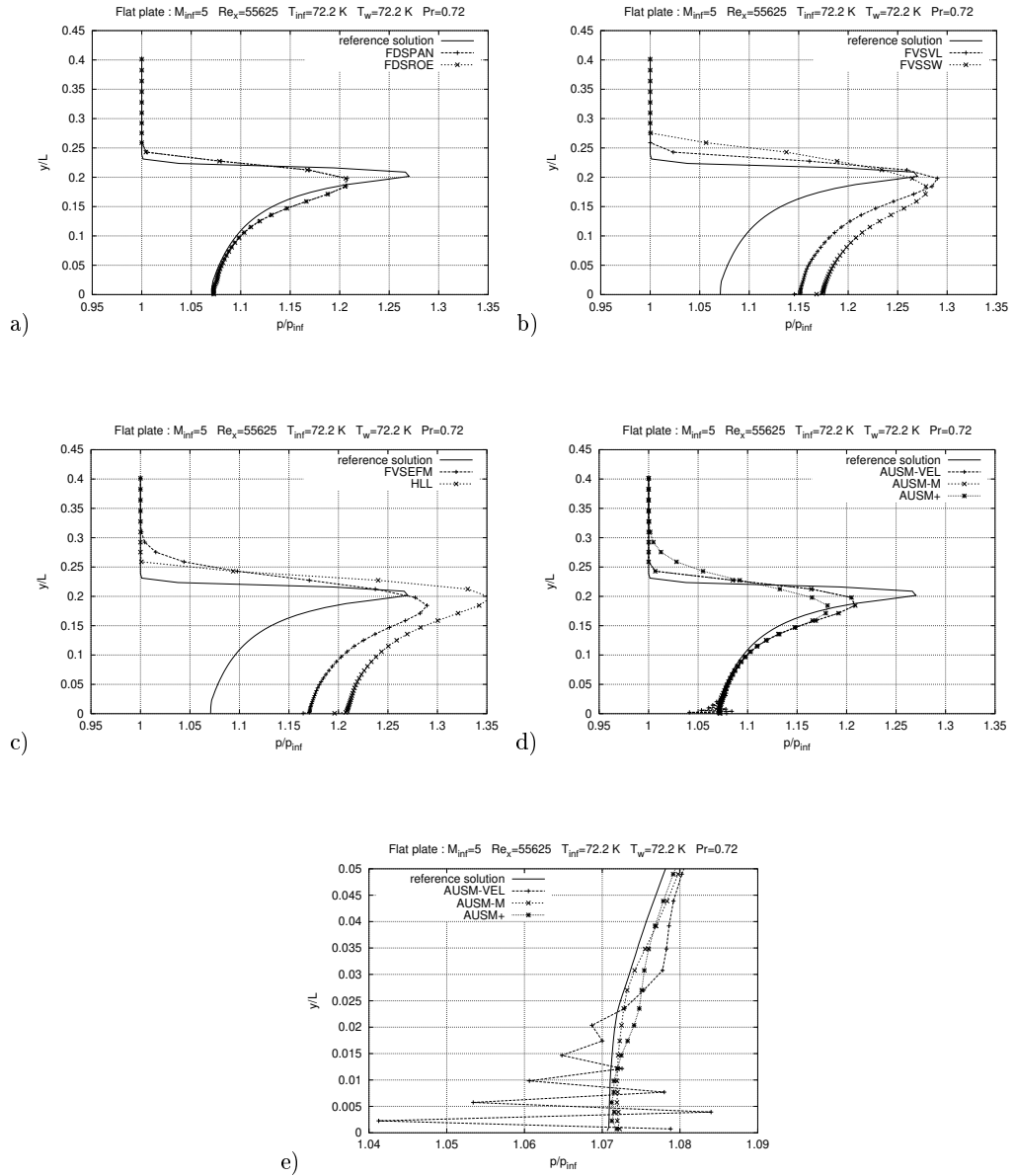


Fig. 1. Pressure plot at $x = 0.89$ m; a) FDSPAN and FDSROE; b) FVSVL and FVSSW; c) FVSEFM and HLL; d) AUSM-VEL, AUSM-M and AUSM+; e) enlarged view of AUSM-VEL, AUSM-M and AUSM+ behavior close to the wall.